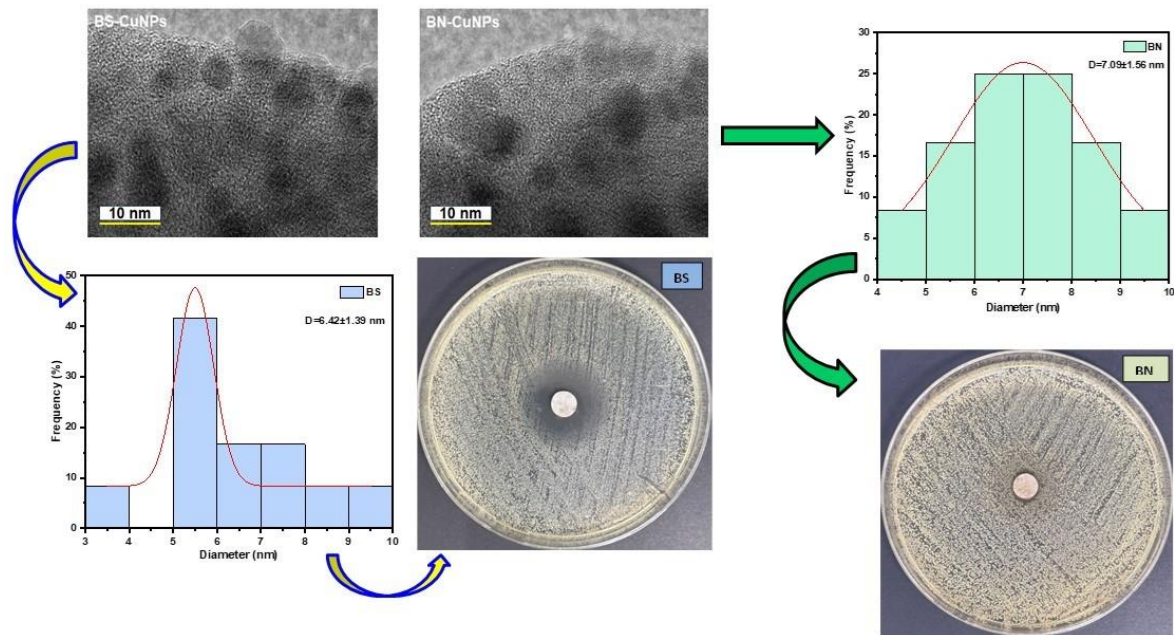# Green Synthesis of Copper Nanoparticles Using White Tea Leaf Extract: Characterization, Adsorption Behavior, and Antibacterial Applications

Zechun Huang,[a,b] Wenchang Zhao,[b,*] Xiyao Liu,[b] Miao Zhong,[b] Xin Ye,[b] and Tzu-Hsing Ko [b,*]

Corresponding author: wenchangzhao@foxmail.com; hsingko@gmail.com

GRAPHICAL ABSTRACT

Green Synthesis of Copper Nanoparticles Using White Tea Leaf Extract: Characterization, Adsorption Behavior, and Antibacterial Applications

Zechun Huang,[a,b] Wenchang Zhao,[b,*] Xiyao Liu,[b,] Miao Zhong,[b] Xin Ye,[b] and Tzu-Hsing Ko [b,*]

Biosynthesis of metal nanoparticles is a cost-effective and environmentally friendly technology. In the present study, copper nanoparticles (CuNPs) were synthesized using white tea leaf extracts. They were then characterized for their chemical structure and evaluated ability for the methylene blue (MB) degradation in the adsorption system with H_2O_2. XRD and FTIR analyses revealed that the CuNPs were present as an amorphous phase, with the O-H polyphenol compound bound to the Cu ion. The XPS deconvolution indicated the presence of Cu^{2+} and Cu^+ in the CuNPs. TEM images revealed that the average particle size was less than 10 nm. The CuNPs synthesized using different precursors exhibited effective ability for the MB degradation in the adsorption system. Based on the adsorption theory, the pseudo-second-order model fitted well with the experimental data, and the thermodynamic calculation suggested that the reaction was endothermic, and spontaneous. The CuNPs synthesized using the $CuSO_4$ precursor exhibited higher antibacterial activity compared to those synthesized using $Cu(NO_3)_2$. In conclusion, white tea leaf extract is an inexpensive and easily available precursor for the biosynthesis of copper nanoparticles. Further analysis based on an assumed degradation work will be considered in future work.

Contact information: a: College of Chemistry and Materials Science, Fujian Normal University, Fuzhou city, China b: Fujian Provincial University Key Laboratory of Featured Biochemical and Chemical Materials, College of New Energy and Materials, Ningde Normal University, Ningde city, China;
* Corresponding author: wenchangzhao@foxmail.com; hsingko@gmail.com

INTRODUCTION

Nanotechnology has been consistently mentioned as a leading technology in global research (Muhammad 2022; Padmanabhan 2023). It is used in electrical, medical, biological, and agricultural fields. Nanoparticles, with dimensions ranging from 1 to 100 nm, exhibit altered physical and chemical properties including shape, size, and composition (Gurunathan *et al*. 2009). Currently, considerable research is focused on exploring the synthesis of nanomaterials using biomass as a subject of widespread interest.

Bio-nanotechnology is well-recognized to utilize organic substances, plant polysaccharides, or polyphenols as the basis for redox reactions. These plant materials offer several advantages, such as productivity, eco-friendliness, a wide range of sources, and cost-effectiveness. Recent studies have reported the economic benefits of using green processes involving plant extracts for the synthesis of nanoparticles, such as ZnO, Ag,

Cu/CuO, Fe^0, MgO, and Co_3O_4 nanoparticles (Pugazhendhi *et al*. 2019; Rama *et al*. 2020; Hao *et al*. 2021; Chakraborty *et al*. 2022; Parvathalu *et al*. 2023; Safdar *et al*. 2023; Vieira *et al*. 2023). These studies elucidate that the green synthesis process remains a popular subject in recent years.

Copper is of great interest in the field of nanotechnology. It is one of the most important trace elements for both plants and animals and is essential for growth in these organisms. In addition, copper is a p-type semiconductor with unique optical, thermally conductive, magnetic, mechanical, and electrical properties, all of which are extensively used in various applications, including catalysis, ceramics, sensors, electronics, and pigments (Kanninen *et al*. 2008; Magdassi *et al*. 2010; Rafique *et al*. 2017; Zhao *et al*. 2020; Mohammed *et al*. 2023; Slimane *et al*. 2023). Copper also exhibits significant bioactive properties and has high biocompatibility and non-toxicity, rendering it potentially suitable for medical and pharmaceutical applications.

For purposes of discussion within this article, the term CuNPs will be used to describe a range of copper-based nanoparticles having chemical compositions that possibly include different oxides or zero-valent copper metal. Pérez-Alvarez *et al*. (2021) used cotton textile fibers to synthesize CuNPs, and this approach offers the benefit of eliminating the use of toxic chemical-based reducing agents. Thakur *et al*. (2018) evaluated the effectiveness of the root and leaf extracts of *Asparagus adscendens* Roxb in the synthesis of CuNPs. They stated that some pathogenic bacteria could be scientifically avoided. Amjad *et al*. (2021) reported the successful synthesis of CuNPs using the extract from *Fortunella margarita* leaves. Ananda *et al.* (2021) reported the synthesis of CuNPs using a medicinal plant named *Vernonia amygdalina.*

In addition, the use of nanocopper materials could reduce the adverse impact of agriculture on the environment (White and Unrine 2019). Based on the high-throughput experiments, it has been discovered that the CuNPs exhibit lower toxicity towards soil and water compared to Cu^{+2} (Keller *et al.* 2017). Moreover, trace copper nanoparticles exert a favorable effect on the regulation of soil microorganisms and plant growth (Qu *et al.* 2022). The relevant literature indicates that the environmental behavior of CuNPs and its toxic effects on soil and water are influenced by various factors, such as pH, temperature, ultraviolet light, and minerals, *etc*. However, after a certain degree of enrichment in the environment, the CuNPs exert a negative impact on aquatic plants, animal cells, soil microorganisms, and the overall environment (He *et al.* 2020; Fu 2021).

Nanomaterials are ideal for applications in the treatment of dye wastewater. Dye wastewater is being generated in increasing amounts in various nations owing to economic development and the increasing demands of the residents. This has led to serious environmental issues, which have not been resolved so far through a proper treatment approach. The dyeing industry is known to be water-intensive with complex dye processing, which exerts a negative impact on human and aquatic lives (Vasantharaj *et al*. 2019; Kumar 2021; Rahimi and Alihosseini 2022).

White tea originates primarily and is mainly produced in the eastern region of Fujian Province. It is a unique type of tea with a relatively high concentration of polyphenols compared to black tea and dark tea, and it has the simplest manufacturing processes. The previous studies by the authors' research group have confirmed that the used black tea, oolong tea, and tea stem may be employed as effective adsorbents for the adsorption of dyes from the aqueous phase after the treatment of the extract (Hu *et al*. 2019; Lin *et al*. 2020; Liu *et al*. 2023). These tea extracts may be used as potential bioactive species for the biosynthesis of metal nanoparticles. These advantages related to the multiple

functions of tea extracts and their biomass in a solid state demonstrates the potential of tea waste for environmental applications. The use of the extract from white tea for the synthesis of CuNPs has not been reported, to the best of the author's knowledge, in any previous study. Therefore, the present study aimed to explore the viability of synthesizing CuNPs using white tea leaf extract and evaluating their structural properties, and adsorption activity. The main objectives were to achieve a complete enrichment of tea waste for the synthesis of metal nanoparticles and their possible applications.

EXPERIMENTAL

Materials

All the chemical reagents used in this study were of analytical grade. Anhydrous $CuSO_4$ and $Cu(NO_3)_2 \cdot 3H_2O$ were purchased from Sinopharm Chemical Reagent Co., Ltd. (Shanghai, China). The methylene blue was from Changde Bickman Biotechnology Co., Ltd. (Changde, China). The H_2O_2 was obtained from Xilong Technology Co., Ltd. (Beijing, China). White tea leaves were provided by the local tea market in Ningde City, Fujian Province (Tiecha Tea Company).

Synthesis of Copper Nanoparticles

Fifty grams of the white tea leaves were ground into powder. The powder was mixed with 1 L of distilled water in a 2 L beaker and stirred for 2 h to obtain the extract. Subsequently, 0.3 mol/L of $CuSO_4$ and $Cu(NO_3)_2$ solution were added to the white tea leaf extract at a volume ratio of 1:2 and stirred homogeneously in a rotary shaker for 12 h. After the reaction, the mixed solutions were centrifuged at 10000 rpm for 5 min to obtain the solid state synthesized Cu-nanoparticles (CuNPs). The synthesized CuNPs were dried in an oven at 353 K for 48 h to obtain dry CuNPs samples. The synthesized CuNPs from $CuSO_4$ were designated as BS, while those from $Cu(NO_3)_2$ were designated as BN in the present study.

Characterization of Copper Nanoparticles

The crystalline structure of CuNPs was analyzed by X-ray powder diffraction (XRD, Bruker D8A-A25) from 5° to 80° at a scanning rate of 1°/min. Fourier transform infrared spectroscopy was used to evaluate the functional groups of the synthesized CuNPs within the range 4000 to 400 cm^{-1} (FTIR, Thermo Scientific Nicolet iS10). Raman spectra were recorded at room temperature in the wavelength range of 200 to 3500 cm^{-1} with the spectral resolution of 10 cm^{-1} using a Raman spectrometer equipped with a He-Ne laser for excitation (Thermo Scientific DXR2 model). The X-ray photoelectron spectrometer (XPS, Thermo Scientific Nexsa) was used to analyze the chemical state of the elements on the surface of CuNPs. The UV spectrophotometer, from Shimadzu Corporation, Japan, was used to determine the absorbance of the MB solution at 667 nm. The distribution and size of CuNPs were characterized by transmission electron microscopy (TEM, Hitachi HT7800), and Nano Measurer 1.2 was used to estimate the size range of particles.

Degradation Experiment

The synthesized CuNPs were evaluated to investigate the degradation of MB in a batch experiment. The adsorption system with/without H_2O_2 was considered. For the adsorption experiment without H_2O_2, 100 mg of CuNPs samples were weighed and mixed

with an MB solution in a liquid-solid ratio of 1 L/g in a conical flask. In the adsorption experiment with H_2O_2, a ratio of 30% H_2O_2 and CuNPs was controlled at 0.01 mL/g under the same conditions as the experiment without H_2O_2. The mixed solution was operated in a thermoregulated shaker at a shaking speed of 200 rpm. After the reaction, the solution was centrifuged at 4000 rpm for 3 min, and the supernatant was analyzed using UV-Vis at 667 nm to determine the MB concentration. The degradation efficiency of MB was calculated using the following equation,

$$\text{Degradation efficiency}(\%) = \frac{C_0 - C_t}{C_0} \times 100 \qquad (1)$$

where C_0 and C_t represent the initial concentration and the MB concentration at any time t, respectively.

Kinetics Model

The pseudo-first-order and second-order kinetic models have been widely used to fit the experimental data for adsorption experiments. The pseudo first-order model can be described by the following linear form (Hubbe *et al*. 2019),

$$\log(Q_e - Q_t) = lnQ_e - \frac{K_{pf}}{2.303}t \qquad (2)$$

where K_{pf} is the constant of the pseudo first-order rate, Q_e is the amount of MG degraded at equilibrium, and Q_t is the amount of MB adsorbed at equilibrium at time t (min).

The pseudo-second order kinetic model is based on the sorption capacity of the solid phase and can be expressed in linear form as shown follows (Ho 2006),

$$\frac{t}{Q_t} = \frac{1}{K_{ps}Q_e^2} + \left(\frac{1}{Q_e}\right)t \qquad (3)$$

where K_{ps} is the constant of the pseudo second-order rate.

Antibacterial Activity

The antibacterial activity of the CuNPs against Gram-positive, *Staphylococcus aureus* (ATCC25923) was evaluated using paper disc diffusion method. A sterile cotton swab was dipped in the prepared bacteria solution with a concentration of 0.5 MCF (McFarland unit, equals to an optical density comparable to the density of a bacterial suspension with a $1.5*10^8$ colony forming units (CFU/mL)) and applied to the entire surface of the Mueller-Hinton broth medium. After the bacterial solution was evenly distributed, the paper containing the BS and BN samples was pasted and taken out to measure the diameter of the inhibition zone after a constant temperature of 310 K for 24 h.

RESULTS AND DISCUSSION

XRD, FTIR, and Raman Analysis of CuNPs

The synthesized Cu-nanoparticle samples were subjected to XRD, FTIR, Raman, and XPS spectroscopic analyses to understand their chemical structures. Both BS and BN exhibited a similar trend, with a noticeable bulge feature at $2\theta = 22°$. This observation could be explained by the fact that the organic compounds from the tea leaf extract were adsorbed as capping or stabilizing agents. This observation was confirmed in the subsequent FTIR analysis as well. In addition, no distinct Cu^0, CuO, or Cu_2O peaks were detected in this study, indicating that the crystal of the synthesized Cu-nanoparticle sample

probably exhibited an amorphous structure. Similar XRD results have also been reported in previous studies (Machado *et al.* 2015; Liu *et al.* 2018). The white tea extract is rich in active biomolecules, which cause the copper ions to become immediately involved in the formation of CuNPs. However, since the standard reduction potential of copper is +0.16 V, not much time might be available for the formation of the crystalline phase of CuNPs in such a reducing medium, resulting in an amorphous form. Similar phenomena have been observed in another report (Ayadi *et al.* 2022). Another possibility is that the samples might have contained quite small amount of zero-valent copper, which was difficult to detect in XRD as well as the subsequent FTIR and Raman analyses.
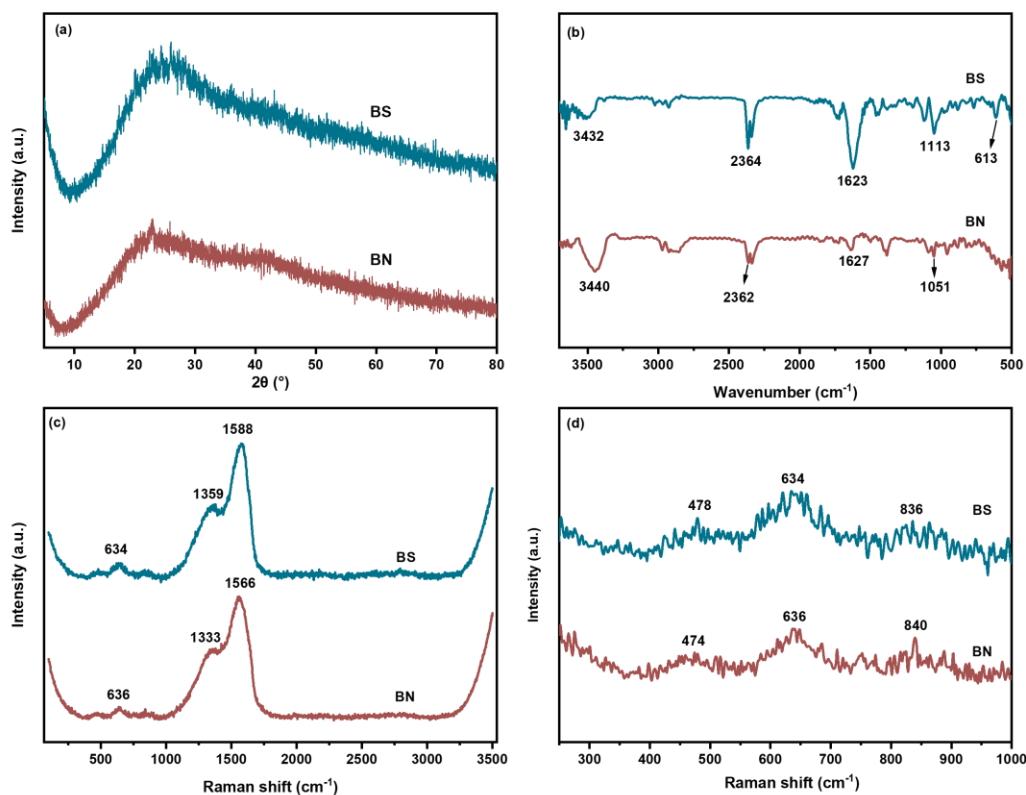

Fig. 1. Spectroscopy patterns of CuNPs (a) XRD (b) FTIR, (c) Raman and (d) Raman local map (250 to 1000 cm^{-1})

The FTIR spectra of the BS and BN samples revealed a similar pattern (Fig. 1b). The absorbance peak appearing at around 3440 cm^{-1} in both samples was attributed to the stretching oscillation of O-H present in the tea polyphenols. The sharp split band at 2362 to 2364 cm^{-1} was observed. This probably can be attributed to CO_2. A false peak can arise when the CO_2 concentration varies between when running the calibration and when running the sample (Taraschewski *et al.* 2005). Further, bands appeared at 1623 to 1627 cm^{-1} corresponded to the C=O stretching of the carbonyl, while the band at 1051 to 1113 cm^{-1} was associated with the in-plane scissoring of CH_2 (Priya and Velraj 2012) or the O-H polyphenol compound bonded to the Cu ion (Duman *et al.* 2016). These observations suggested that the groups bound to the surface of CuNPs were related to the flavonoids present in the white tea leaves (Makwana *et al.* 2014; Sutradhar *et al.* 2014).

Raman spectroscopy is a versatile and sensitive technique for surface analysis to elucidate the chemical interactions and the vibrational properties of materials. The peaks detected at 634 and 635 cm^{-1} corresponded to the typical Bg mode of the Raman active node associated with the symmetric oxygen stretching of Cu-O. Similar observations have been reported in previous studies (Ahmed *et al*. 2013; He *et al*. 2016). Notably strong and broad peaks appeared at 1346 and 1566 cm^{-1}. The peaks that appeared around 1346 and 1355 cm^{-1} corresponded to the feature of disorder, defined as the D-peak, while the peaks appearing around 1566 and 1588 cm^{-1} reflected the first-order scattering of sp^2 carbon atoms and were defined as the G-peak (Li *et al*. 2023). The occurrence of the D and G-peaks was attributed to the presence of tea polyphenols and other carbonaceous bioactive species in the white tea extract, particularly the species that chelate and stabilize the copper to form CuNPs. The intensity ratio (I_D/I_G) of the D and G peaks is normally calculated to reflect the degree of defects in the carbon layers and the degree of covalent modification. In this study, the I_D/I_G values for BS and BN were determined to be 0.423 and 0.462, respectively. These values indicated fewer defects and a more ordered structure. The above observations were consistent with the findings of the XRD analysis, with no distinct diffraction peaks corresponding to the Cu species, although a noticeable hump feature indicated the presence of carbonaceous species. In summary, the CuNPs in the present study had an amorphous form of crystalline phase.
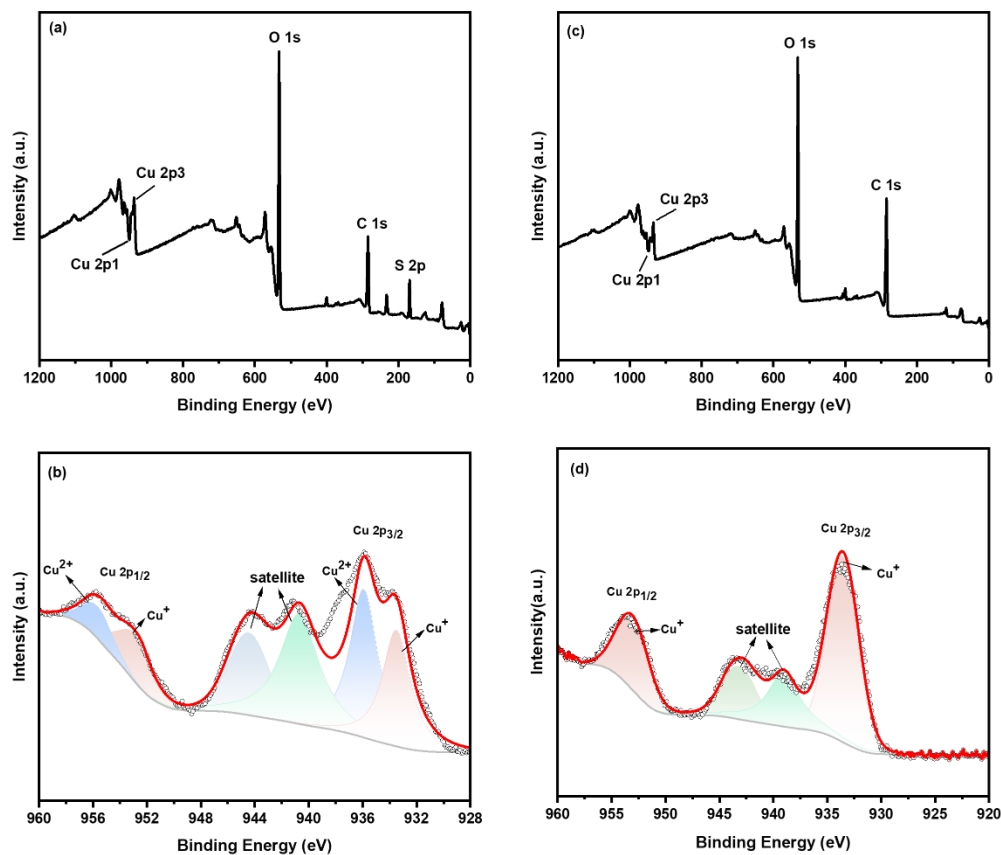

Fig. 2. XPS analysis and deconvolution result (a) wide-range scan of BS (b) Cu 2p fitting of BS (c) wide-range scan of BN, and (d) Cu 2p fitting of BN

XPS Analysis

The BS and BN samples were evaluated for surface elemental composition and electronic state using XPS. The wide-range scan revealed the presence of Cu, O, C, and S as the main elements on the surface of both samples (Figs. 2a-b). As depicted in Fig. 2b, the Cu $2p^{3/2}$ region exhibited doublet peaks and demonstrated the coexistence of Cu^+ at 933.8 eV and Cu^{2+} at 935.9 eV after deconvolution. Moreover, the peaks were detected at 941.2 to 944.5 eV, belonging to the shake-up satellite and interpreted the presence of the paramagnetic chemical states of Cu^{2+}.

The characteristics peak of 953.8 cm^{-1} in the Cu $2p^{1/2}$ region appeared with a binding energy gap close to 19.9 eV between the peaks of Cu $2p^{3/2}$, providing further evidence for the formation of CuO (Siddiqui *et al*. 2020). Unlike the BS sample, the BN sample presented no significant split peaks in the Cu $2p^{3/2}$ and Cu $2p^{1/2}$ regions. The intensity of the satellite peak of the BN sample was weaker than that of the BS sample. In particular, the satellite peaks shifted to 940.2 and 942.8 eV, which was slightly lower than those of the BS sample. These findings indicated that Cu^+ was the most important species in the BN sample.

TEM Analysis of CuNPs

The TEM images revealed that the synthesized CuNPs had a spherical structure, with an average size of 6.42 nm noted for the BS sample, and 7.09 nm for the BN sample (Fig. 3). The TEM images confirmed the feasibility of biosynthesizing CuNPs from white tea extract and achieving the nanostructure of CuNPs, as reported in the present study.
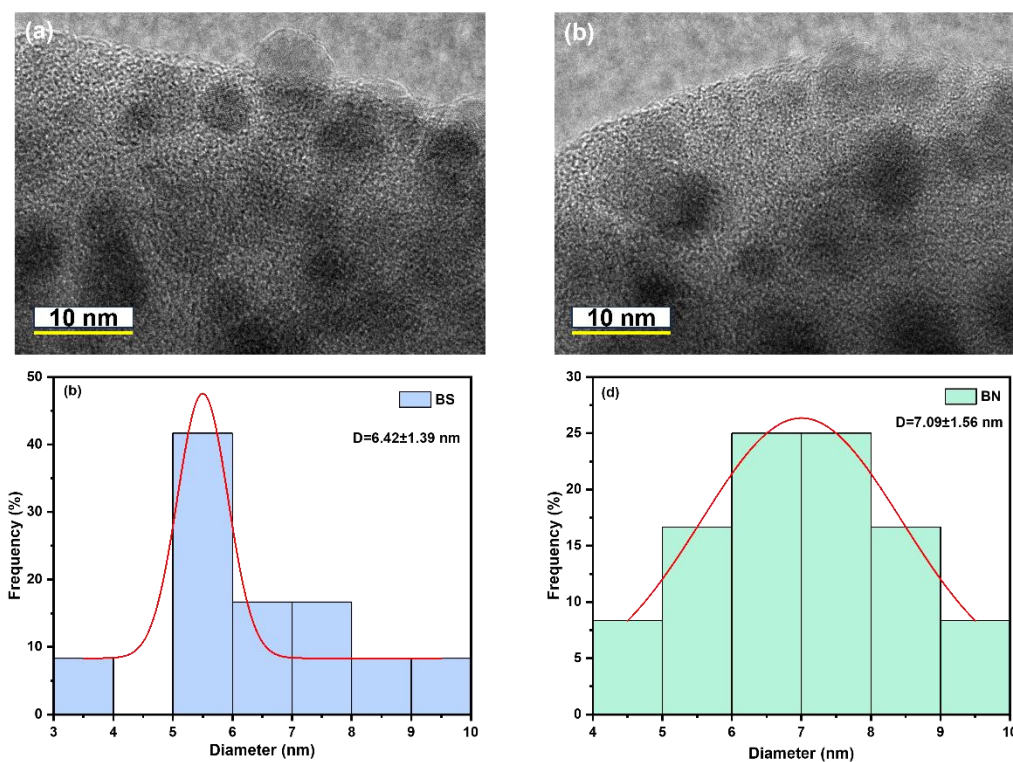

Fig. 3. TEM images of (a) BS sample and (c) BN sample and grain size distribution histogram of (b) BS sample and (d) BN sample

Degradation of MB for Synthesized CuNPs

The application of the synthesized CuNPs to the degradation of MB together with sole adsorption was evaluated (Figs. 4a and 4b). It was found that less than 50% of the degradation efficiency was achieved at 30 min in the sole adsorption for both samples. The degradation efficiency of MB increased with reaction time, and at 60 min, the values of approximately 75% and 73% were reached for the BS and BN samples, respectively. A slight increase in the degradation efficiency was observed for the BN sample, while the BS sample exhibited much higher degradation efficiency. This observation indicated that the interaction between the MB molecules and the synthesized CuNPs in the present study was favorable and that both the samples exhibited adsorption affinity for MB. On the other hand, in adsorption system with H_2O_2, a rapid degradation efficiency of approximately 70% and 40% was achieved for the BS and BN samples, respectively, after 5 min. After 60 min, approximately 90% of the degradation efficiency was achieved for the BS sample and nearly 80% degradation efficiency was achieved for the BN sample, which is strong evidence that the CuNPs functioned as effective catalysts for the degradation of MB molecules under the experimental conditions. Further evaluation of the effect of different H_2O_2 concentrations on the efficiency of the two samples revealed that the degradation efficiency increased with the increasing H_2O_2 concentration for both samples (Figs. 5a and 5b). The higher the H_2O_2 concentration, the greater the number of hydroxyl radicals that are formed, and consequently, the greater the driving force for the degradation of MB molecules over the CuNPs.

In order to understand the effects of reaction temperature, experiments were conducted at different temperatures in the range of 278 to 318 K. The degradation efficiency was observed to increase from 83% to 95% for the BS sample and from 76% to 93% for the BN sample at 120 min, when the temperature was increased from 278 to 318 K (Figs. 6a and 6b). The following could be the reasons for this result: (i) the kinetic energy of MB molecules increased at a higher temperature, promoting the collision frequency between the active sites of CuNPs, and (ii) a higher reaction temperature accelerated the rate of hydroxyl radicals generation from H_2O_2 in the presence of CuNPs. As described above, under experimental conditions, both BS and BN samples exhibited acceptable levels of degradation of MB in this study.
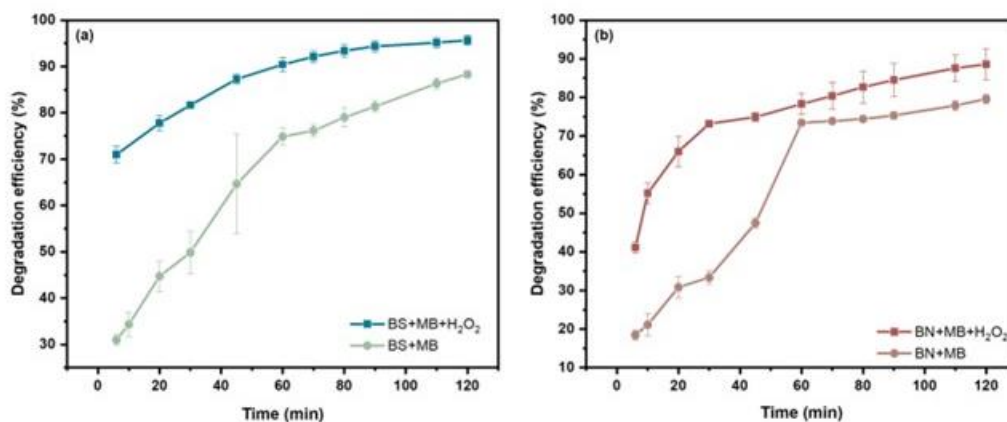

Fig. 4. Degradation of MB for the synthesized CuNPs in different reaction system (a) BS sample (b) BN sample
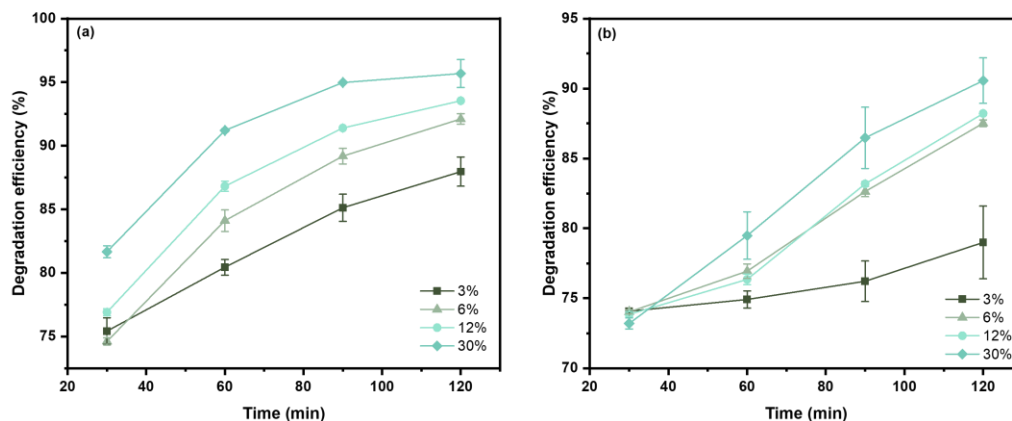
Fig. 5. Degradation of MB for the synthesized CuNPs in different H_2O_2 concentrations (a) BS sample (b) BN sample
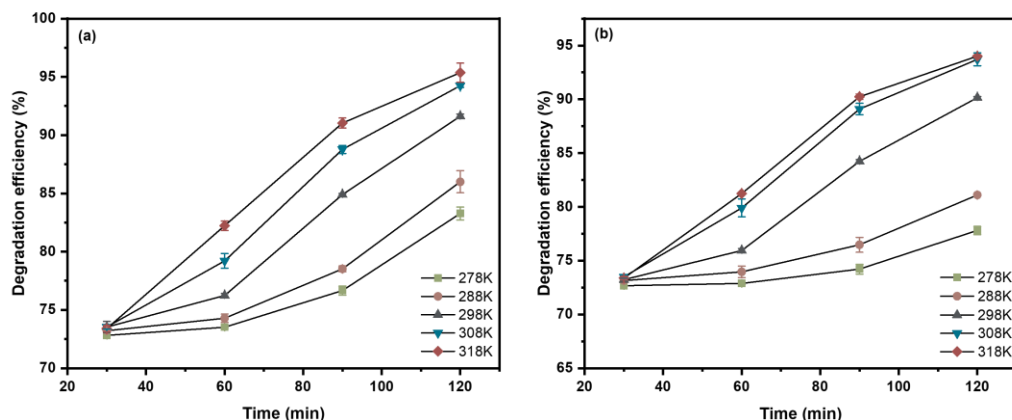

Fig. 6. Degradation of MB for the synthesized CuNPs at different reaction temperatures (a) BS sample (b) BN sample

Kinetics of CuNPs

The kinetic relationships for the adsorption of MB using BS and BN samples were determined based on pseudo-first-order and pseudo-second-order models. The fitting results of the kinetic models are presented in the Fig. 7 and Table 1. The pseudo-second-order model presented a strong fit, with a coefficient of determination of over 0.998, while the pseudo-first-order model showed relatively lower correlation. The calculated adsorption capacities (Q_{max}) for the BS and BN samples were 19.3 and 26.4 mg/g, respectively, in the pseudo-first-order model and 49.7 and 46.9 mg/g, respectively, in the pseudo-second-order model.

The Q_{max} values calculated for the pseudo-second-order model agreed well with the experimental values (Q_{exp}), indicating the superiority of the pseudo-second-order model in predicting the kinetic of the MB degradation. The favorable fits to the pseudo-second-order model elucidated that the rate of adsorption was determined by the diffusion of dye molecules within a network of very small pores (Hubbe *et al.* 2019).
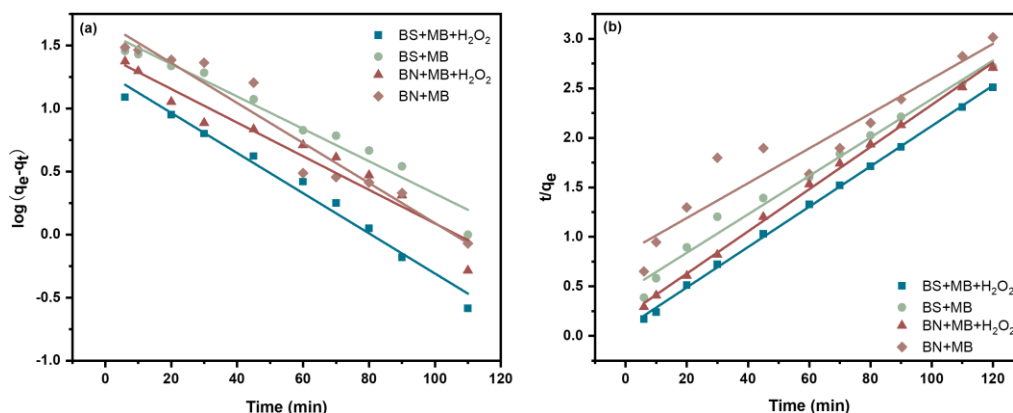
Fig. 7. Linear fitting plots of (a) pseudo-first-order, (b) pseudo-second-order model for the adsorption of MB

Table 1. Kinetics Parameters of the Adsorption of MB by CuNPs

Condition	Pseudo-first-order				Pseudo-second-order		
	Q_{exp} (mg/g)	K_1 (1/min)	R^2	Q_{max} (mg/g)	K_2 (1/min)	R^2	Q_{max} (mg/g)
$BS+MB+H_2O_2$	47.837	0.037	0.979	19.271	0.005	0.999	49.068
$BN+MB+H_2O_2$	44.304	0.031	0.931	26.442	0.002	0.998	46.948

Thermodynamic Investigation

Thermodynamic analysis can provide valuable insights into the spontaneous condition of the reaction. Thermodynamic parameters are calculated based on the third law of thermodynamics. The equilibrium constant of CuNPs is calculated at different temperatures, assuming that CuNPs is in an equilibrium state. The change in Gibb's free energy is used to determine the thermodynamic parameters shown as following equations,

$$\triangle G^0 = R\,T\,ln\,K \tag{4}$$

$$ln\,K = -\frac{\triangle H^0}{RT} + \frac{\triangle S^0}{R} \tag{5}$$

where ΔG^0 is the standard Gibbs free energy, and R is the gas constant. T is the absolute temperature, and K is the rate constant of reaction at the equilibrium state. The enthalpy (ΔH^0) and entropy (ΔS^0) can be calculated from the slope and intercept of the linear straight by plotting $ln\,K$ versus $1/T$.

The calculated thermodynamic parameters for BS and BN samples at different temperatures are listed in Table 2. The ΔG^0 values calculated at different temperatures were negative for both samples and ranged from -1.48 to -3.19 KJ/mol for the BS sample and from -1.19 to -3.03 KJ/mol for the BN sample. The value of ΔG^0 decreased with increasing temperature, indicating that the interaction between MB, H_2O_2, and CuNPs is a favorable and feasible degradation process that occurs spontaneously with an endothermic reaction over the temperature ranges of 278 to 318 K. The positive ΔS^0 values were noted for both BS and BN samples, which indicates an increase in disorder at the interface between MB and the CuNPs.

Table 2. Thermodynamic Parameters of Synthesized CuNPs at Different Temperatures for Adsorption of MB

T(K)	ΔG^0 (kJ/mol)		ΔH^0 (kJ/mol)		ΔS^0 (kJ/mol·K)	
	BS	BN	BS	BN	BS	BN
278	-1.479	-1.194				
288	-1.781	-1.390				
298	-2.427	-2.249	6.917	4.255	0.030	0.020
308	-2.854	-2.758				
318	-3.186	-3.030				

Antibacterial Activity of the Synthesized CuNPs

The antibacterial activity of the synthesized CuNPs was evaluated against *Staphylococcus aureus* using the disk diffusion test, which revealed different results (Fig. 8). The BS sample exhibited a higher antibacterial ability with an inhibition zone of 12 mm, while the BN sample led to an inhibition zone of just 2 mm. Several studies have indicated that metal ions released from nanoparticles can bind to the negatively charged bacterial cell wall, leading to cell wall rupture. In addition, these particle ions may interact with the DNA and protein biomolecules, leading to a crosslinking process that distorts the helical DNA and protein structures, thereby disrupting the essential biochemical processes occurring in the body (Kim *et al.* 2011). The antibacterial ability of a material depends on the particle size and the ion release rate as they are more easily adsorbed and have a larger surface area (Azam *et al.* 2012). Skandalis *et al*. (2017) used the leaf extracts of *Arbutus unedo* to synthesize the Ag particles sizes of 40 nm and 58 nm. The antibacterial activity showed that the bacterial membrane was destroyed after 10 h of interaction with a particle size of 40 nm, while 58 nm nanoparticles destroyed the membrane after 24 h. The similar trend can be found for Zn and Cu nanoparticles in other reports (Álvarez-Chimal *et al*. 2022; Lai *et al*. 2022). In the present study, the average particle size of BS sample was estimated to be 6.42 and 7.09 nm for the BN sample, respectively. In comparison to the BN sample, the BS sample exhibited a smaller particle size than the BN sample, leading to an effective antibacterial ability.
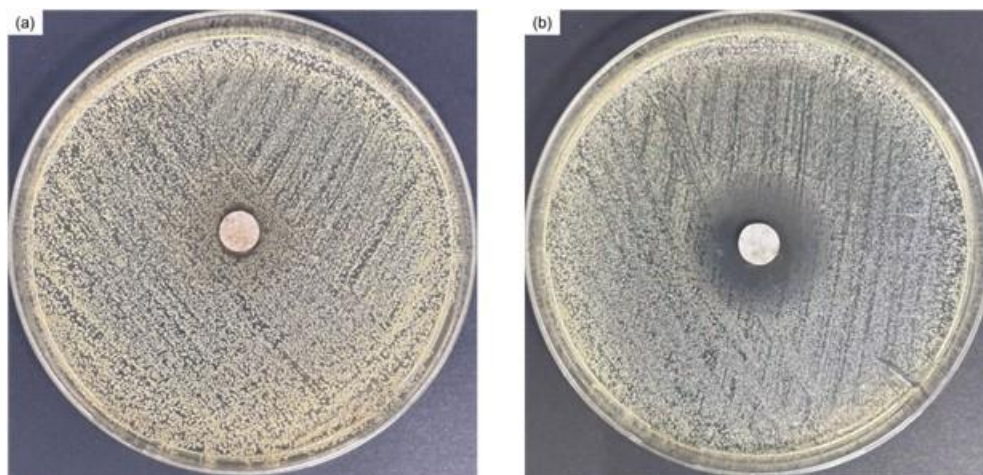
Fig. 8. Antibacterial activity of (a) BN and (b) BS against *Staphylococcus aureus*

CONCLUSIONS

1. Green synthesis of copper-based nanoparticles (CuNPs) using white tea extract presented a spherical structure with a size between 6.42 and 7.09 nm. X-ray photoelectron spectrometry (XPS) demonstrated the presence of Cu^{2+} and Cu^+ in the CuNPs.

2. The synthesized CuNPs exhibited the ability to decrease the concentration of MB in solution. Two kinds of mechanisms were considered to account for such results. First, the kinetic data and temperature-dependent equilibrium adsorption capacities were consistent with diffusion-controlled adsorption of the MB onto the CuNPs. Secondly, future work might consider whether or not the data could be fitted to equations based on the catalytic degradation of the MB. The temperature-dependence indicated that the process was thermodynamically favorable and that it occurred spontaneously as an endothermic reaction.

3. CuNPs synthesized using $CuSO_4$ exhibited antibacterial activity against *Staphylococcus aureus.*

ACKNOWLEDGMENTS

REFERENCES CITED

Álvarez-Chimal, R., García-Pérez, V., Álvarez-Pérez, M. A., Tavera-Hernández, R., Reyes-Carmona, L., Martínez-Hernández, M., and Arenas-Alatorre, J, A. (2022). "Influence of the particle size on the antibacterial activity of green synthesized zinc oxide nanoparticles using *Dysphania ambrosioides* extract, supported by molecular docking analysis," *Arabian Journal of Chemistry* 15(6), article 103804. DOI: 10.1016/j.arabjc.2022.10380

Ahmed, M., Rüsing, M., Berth, G., Lischka, K., and Pawlis, A. (2013). "CuO and Co_3O_4 nanoparticles: Synthesis, characterizations, and Raman spectroscopy," *Journal of Nanomaterials* 2013. DOI: 10.1155/2013/714853

Amjad, R., Mubeen, B., Ali, S. S., Imam, S. S., Alshehri, S., Ghoneim, M. M., Alzarea, S. I., Rasool, R., Ullah, I., Nadeem, M. S., and Kazmi, I. (2021). "Green synthesis and characterization of copper nanoparticles using *Fortunella margarita* leaves," *Polymers (Basel)* 13(24), article 4364. DOI: 10.3390/polym13244364

Ananda, M. H. C., Zeleke, T. D., Tan, K. B., Ghotekar, S., Alam, M. W., Balachandran, R., Chan, K.-Y., Sanaulla, P. F., Anil, K. M. R., and Ravikumar, C. R. (2021). "Enhanced multifunctionality of CuO nanoparticles synthesized using aqueous leaf extract of *Vernonia amygdalina* plant," *Results in Chemistry* 3, article 100141. DOI: 10.1016/j.rechem.2021.100141

Azam, A., Ahmed, A. S., Oves, M., Khan, M. S., Habib, S. S., and Memic, A. (2012). "Antimicrobial activity of metal oxide nanoparticles against Gram-positive and

Gram-negative bacteria: A comparative study," *Int. J. Nanomedicine* 7, 6003-9. DOI: 10.2147/ijn.S35347

Chakraborty, N., Banerjee, J., Chakraborty, P., Banerjee, A., Chanda, S., Ray, K., Acharya, K., and Sarkar, J. (2022). "Green synthesis of copper/copper oxide nanoparticles and their applications: A review," *Green Chemistry Letters and Reviews* 15(1), 187-215. DOI: 10.1080/17518253.2022.2025916

Duman, F., Ocsoy, I., and Kup, F. O. (2016). "Chamomile flower extract-directed CuO nanoparticle formation for its antioxidant and DNA cleavage properties," *Materials Science and Engineering C*, 60, 333-338. DOI: 10.1016/j.msec.2015.11.052

Fu, Y. (2021). *Toxic Effects and Ecological Risks of Copper and Copper Oxide Nanoparticles on Soil and Brassica chinensis L.*, Master's Thesis, Northeast Agricultural University, Heilongjiang Province, China

Gurunathan, S., Kalishwaralal, K., Vaidyanathan, R., Venkataraman, D., Pandian, S. R. K., Muniyandi, J., Hariharan, N., and Eom, S. H. (2009). "Biosynthesis, purification and characterization of silver nanoparticles using *Escherichia coli*," *Colloids and Surfaces B: Biointerfaces* 74(1), 328-335. DOI: 10.1016/j.colsurfb.2009.07.048

Hao, R., Li, D., Zhang, J., and Jiao, T. (2021). "Green synthesis of iron nanoparticles using green tea and its removal of hexavalent chromium," *Nanomaterials (Basel)*, 11(3). DOI: 10.3390/nano11030650

Hassan, S. A., Ghadam, P., and Abdi A. A. (2022). "One step green synthesis of Cu nanoparticles by the aqueous extract of Juglans regia green husk: Assessing its physicochemical, environmental and biological activities," *Bioprocess and Biosystems Engineering* 45(3), 605-618. DOI: 10.1007/s00449-022-02691-2

He, J., Jiang, Y., Peng, J., Li, C., Yan, B., and Wang, X. (2016). "Fast synthesis of hierarchical cuprous oxide for nonenzymatic glucose biosensors with enhanced sensitivity," *Journal of Materials Science* 51(21), 9696-9704. DOI: 10.1007/s10853-016-0202-3

He, Y., Chu, M. W., Liu, Y., Liu, R. Q., Duan, W. Y., and Qiu H. (2020). "Toxicity and the underlying mechanisms of copper and copper oxide nanoparticles to duckweed and algae: A review," *Asian Journal of Ecotoxicology* 15(4), 56-65. DOI: 10.7524/AJE.1673-5897.20190710002

Ho, Y.-S. (2006). "Review of second-order models for adsorption systems," *Journal of Hazardous Materials* 136(3), 681-689. DOI: 10.1016/j.jhazmat.2005.12.043

Hu, Y., Zhang, Y., Hu, Y., Chu, C.-Y., Lin, J., Gao, S., Lin, D., Lu, J., Xiang, P., and Ko, T.-H. (2019). "Application of wasted oolong tea as a biosorbent for the adsorption of methylene blue," *Journal of Chemistry* 2019, article 4980965. DOI: 10.1155/2019/4980965

Hubbe, M., Azizian, S., and Douven, S. (2019). "Implications of apparent pseudo-second-order adsorption kinetics onto cellulosic materials: A review," *BioResources* 14(3), 7582-7626. DOI: 10.15376/biores.14.3.

Kanninen, P., Johans, C., Merta, J., and Kontturi, K. (2008). "Influence of ligand structure on the stability and oxidation of copper nanoparticles," *Journal of Colloid and Interface Science* 318(1), 88-95. DOI: 10.1016/j.jcis.2007.09.069

Keller, A. A., Adeleye, A. S., Conway, J. R., Garner, K. L., Zhao, L., Cherr, G. N., Hong, J., Gardea-Torresdey, J. L., Godwin, H. A., Hanna, S., Ji, Z., Kaweeteerawat, C., Lin, S., Lenihan, H. S., Miller, R. J., Nel, A. E., Peralta-Videa, J. R., Walker, S. L., Taylor, A. A., Torres-Duarte, C., Zink, J. I., and Zuverza-Mena, N. (2017). "Comparative environmental fate and toxicity of copper nanomaterials," *NanoImpact* 7, 28-40. DOI:

10.1016/j.impact.2017.05.003

Kim, S. H., Lee, H. S., Ryu, D. S., Choi, S. J., and Lee, D. S. (2011). "Antibacterial activity of silver-nanoparticles against *Staphylococcus aureus* and *Escherichia coli*," *Microbiology and Biotechnology Letters* 39(1), 77-85.

Kumar, B. (2021). "Green synthesis of gold, silver, and iron nanoparticles for the degradation of organic pollutants in wastewater," *Journal of Composites Science* 5(8). DOI: 10.3390/jcs5080219

Lai, M. J., Huang, Y. W., Chen, H. C., Tsao, L. I., Chang-Chien C. F., Singh, B., and Liu, B. R. (2022). "Effect of size and concentration of copper nanoparticles on the antimicrobial activity in *Escherichia oli* through multiple mechanisms," *Nanomaterials* 12(21), article 3715. DOI: 10.3390/nano12213715

Li, D., Shao, Y., Ke, H., Chang, S., Kou, Y., Xiao, L., and Hao, G. (2023). "Synthesis of covalently modified energetic graphene oxide/CuO composites with enhanced catalytic performance for thermal decomposition of ammonium perchlorate," *ACS Omega* 8(25), 22876-22886. DOI: 10.1021/acsomega.3c01865

Lin, D., Wu, F., Hu, Y., Zhang, T., Liu, C., Hu, Q., Hu, Y., Xue, Z., Han, H., and Ko, T.-H. (2020). "Adsorption of dye by waste black tea powder: Parameters, kinetic, equilibrium, and thermodynamic studies," *Journal of Chemistry* 2020, article 5431046. DOI: 10.1155/2020/5431046

Liu, X., Wu, Y., Zhao, W., Wu, Z., Han, H., Xie, Z., Yilmaz, M., and Ko, T.-H. (2023). "Adsorption of malachite green from aqueous phase by tea stalk powder: Parameters, kinetic, isothermal, and thermodynamic studies," *BioResources* 18(3), 6364-6383. DOI: 10.15376/biores.18.3.6364-6383

Liu, Y., Jin, X., and Chen, Z. (2018). "The formation of iron nanoparticles by *Eucalyptus* leaf extract and used to remove Cr(VI)," *The Science of the Total Environment* 627, 470-479. DOI: 10.1016/j.scitotenv.2018.01.241

Machado, S., Pacheco, J. G., Nouws, H. P. A., Albergaria, J. T., and Delerue-Matos, C. (2015). "Characterization of green zero-valent iron nanoparticles produced with tree leaf extracts," *Science of The Total Environment* 533, 76-81. DOI: 10.1016/j.scitotenv.2015.06.091

Magdassi, S., Grouchko, M., and Kamyshny, A. (2010). "Copper nanoparticles for printed electronics: routes towards achieving oxidation stability," *Materials (Basel)*, 3(9), 4626-4638. DOI: 10.3390/ma3094626

Makwana, D. B., Parikh, P., and Zala, D. (2014). "Biosynthesis of copper nanoparticles and their antimicrobial activity," *OALib Journal* 1, 1-15. DOI: 10.4236/oalib.preprints.1200067

Mohammed, Y. A. P., Muthukrishnan, R. M., Imran, K. R., Vedhi, C., Sakthipandi, K., and Abdul, K. S. M. (2023). "Green synthesis of copper oxide nanoparticles using *Amaranthus dubius* leaf extract for sensor and photocatalytic applications," *Chemical Physics Impact* 7, article 100374. DOI: 10.1016/j.chphi.2023.100374

Muhammad, I. D. (2022). "A comparative study of research and development related to nanotechnology in Egypt, Nigeria and South Africa," *Technology in Society* 68, article 101888. DOI: 10.1016/j.techsoc.2022.101888

Padmanabhan, S. (2023). "Nanotechnology in orthodontics," *Seminars in Orthodontics*, 29(1), 79-84. DOI: 10.1053/j.sodo.2023.01.005

Parvathalu, K., Kumar, D. N., Rajitha, K., Kishan, M. G., Kumar, B. N., Bhemarajam, J., Naidu, S. R., Merlinsheeba, G. L., Mandal, P., Banne, S., Dayanand, A., Morampudi, V., Murali, B., Vinodini, S. E. N., Reddy, Y. V., and Bhaskar, P. B. (2023). "Facile

synthesis of silver nanoparticles using green tea leaf extract and evolution of antibacterial activity," *Plasmonics* 18(5), 1837-1845. DOI: 10.1007/s11468-023-01899-6

Pérez-Alvarez, M., Cadenas-Pliego, G., Pérez-Camacho, O., Comparán-Padilla, V. E., Cabello-Alvarado, C. J., and Saucedo-Salazar, E. (2021). "Green synthesis of copper nanoparticles using cotton," *Polymers (Basel)* 13(12), article 1906. DOI: 10.3390/polym13121906

Priya, C. S., and Velraj, G. (2012). "Synthesis and characterization of nano and micro copper doped conducting polymer," *Materials Letters* 77, 29-31. DOI: 10.1016/j.matlet.2012.02.112

Pugazhendhi, A., Prabhu, R., Muruganantham, K., Shanmuganathan, R., and Natarajan, S. (2019). "Anticancer, antimicrobial and photocatalytic activities of green synthesized magnesium oxide nanoparticles (MgONPs) using aqueous extract of *Sargassum wightii*," *Journal of Photochemistry and Photobiology B: Biology* 190, 86-97. DOI: 10.1016/j.jphotobiol.2018.11.014

Qu, H., Ma, C., Xing, W., Xue, L., Liu, H., White, J. C., Chen, G., and Xing, B. (2022). "Effects of copper oxide nanoparticles on Salix growth, soil enzyme activity and microbial community composition in a wetland mesocosm," *Journal of Hazardous Materials* 424, article 127676. DOI: 10.1016/j.jhazmat.2021.127676

Rafique, M., Sadaf, I., Rafique, M. S., and Tahir, M. B. (2017). "A review on green synthesis of silver nanoparticles and their applications," *Artificial Cells, Nanomedicine, and Biotechnology* 45(7), 1272-1291. DOI: 10.1080/21691401.2016.1241792

Rahimi, A. A., and Alihosseini, F. (2022). "Application of dye saturated clay adsorbent from dyeing wastewater as textile printing pigment," *Journal of Chemical Technology & Biotechnology* 97(11), 3152-3162. DOI: 10.1002/jctb.7183

Rama, K. A. G., Espenti, C. S., Rami, R. Y. V., Obbu, A., and Satyanarayana, M. V. (2020). "Green synthesis of silver nanoparticles by using *Sansevieria roxburghiana*, their characterization and antibacterial activity," *Journal of Inorganic and Organometallic Polymers and Materials* 30(10), 4155-4159. DOI: 10.1007/s10904-020-01567-w

Safdar, A., Mohamed, H. E., Hkiri, K., Muhaymin, A., and Maaza, M. (2023). "Green synthesis of cobalt oxide nanoparticles using *Hyphaene thebaica* fruit extract and their photocatalytic application," *Applied Sciences* 13(16). DOI: 10.3390/app13169082

Siddiqui, H., Qureshi, M. S., and Haque, F. Z. (2020). "Biosynthesis of flower-shaped CuO nanostructures and their photocatalytic and antibacterial activities," *Nano-Micro Letters* 12(1), 29. DOI: 10.1007/s40820-019-0357-y

Skandalis, N., Dimopoulou, A., Georgopoulou, A., Gallios, N., Papadopoulos, D., Tsipas, D., Theologidis, I., Michailidis, N., and Chatzinikolaidou, M. (2017). "The effect of silver nanoparticles size, produced using plant extract from *Arbutus unedo*, on their antibacterial efficacy, " *Nanomaterials* 7(7), 178. DOI: 10.3390/nano7070178

Slimane, B. A. D., Krid, F., Nacef, M., Boussaha, E. H., Chelaghmia, M. L., Tabet, H., Selaimia, R., Atamnia, A., and Affoune, A. M. (2023). "Green synthesis of copper oxide nanoparticles using *Ficus elastica* extract for the electrochemical simultaneous detection of Cd^{2+}, Pb^{2+}, and Hg^{2+}," *RSC Advances* 13(27), 18734-18747. DOI: 10.1039/d3ra02974c

Sutradhar, P., Saha, M., and Maiti, D. (2014). "Microwave synthesis of copper oxide

nanoparticles using tea leaf and coffee powder extracts and its antibacterial activity," *Journal of Nanostructure in Chemistry* 4. DOI: 10.1007/s40097-014-0086-1

Taraschewski, M., Cammenga, H. K., Tuckermann, R., and Bauerecker, S. (2005). "FTIR study of CO_2 and H_2O/CO_2 nanoparticles and their temporal evolution at 80 K," *Journal of Physical Chemistry A*, 109(15), 3337-3343. DOI:10.1021/jp044075r

Thakur, S., Sharma, S., Thakur, S., and Rai, R. (2018). "Green synthesis of copper nano-particles using *Asparagus adscendens Roxb*. root and leaf extract and their antimicrobial activities," *International Journal of Current Microbiology and Applied Sciences* 7(4), 683-694. DOI: 10.20546/ijcmas.2018.704.077

Vasantharaj, S., Sathiyavimal, S., Senthilkumar, P., LewisOscar, F., and Pugazhendhi, A. (2019). "Biosynthesis of iron oxide nanoparticles using leaf extract of *Ruellia tuberosa*: antimicrobial properties and their applications in photocatalytic degradation," *Journal of Photochemistry and Photobiology B: Biology* 192, 74-82. DOI: 10.1016/j.jphotobiol.2018.12.025

Vieira, I. R. S., da Silva, A. A., da Silva, B. D., Neto, L. T., Tessaro, L., Furtado, C. R. G., de Sousa, A. M. F., Carvalho, N. M. F., and Conte-Junior, C. A. (2023). "Eco-friendly synthesis of ZnO nanomaterial from green tea extract: photocatalytic, antibacterial and antioxidant potential," *Biomass Conversion and Biorefinery*. DOI: 10.1007/s13399-023-04456-7

White, J. C., and Unrine, J. M. (2019). "Foreword to the research front on 'Nanotechnology and Agriculture' ," *Environmental Chemistry* 16(6), 375-376. DOI: 10.1071/ENv16n6_FO

Zhao, M., Chen, W., Wu, W., Zhang, M., and Li, Z. (2020). "Aging characteristic of Cu-doped nickel manganite NTC ceramics," *Journal of Materials Science: Materials in Electronics* 31(14), 11784-11790. DOI: 10.1007/s10854-020-03730-y